THE JOURNAL OF BIOLOGICAL CHEMISTRY VOL. 281, NO. 37, pp. 27471–27480, September 15, 2006

Engineering ATPase Activity in the Isolated ABC Cassette of Human TAP1*

Received for publication, February 6, 2006, and in revised form, June 30, 2006 Published, JBC Papers in Press, July 24, 2006, DOI 10.1074/jbc.M601131200

Robert Ernst[‡], **Joachim Koch**[§], **Carsten Horn**[‡1], **Robert Tampé**[§], **and Lutz Schmitt**[‡2]

From the [‡]*Institute of Biochemistry, Heinrich Heine University Duesseldorf, Universitaetsstrasse 1, 40225 Duesseldorf and the* [§]*Institute of Biochemistry, Biocenter, Johann-Wolfgang Goethe University Frankfurt, Marie Curie Strasse 9, 60439 Frankfurt, Germany*

The human transporter associated with antigen processing (TAP) translocates antigenic peptides from the cytosol into the endoplasmic reticulum lumen. The functional unit of TAP is a heterodimer composed of the TAP1 and TAP2 subunits, both of which are members of the ABC-transporter family. ABC-transporters are ATP-dependent pumps, channels, or receptors that are composed of four modules: two nucleotide-binding domains (NBDs) and two transmembrane domains (TMDs). Although the TMDs are rather divergent in sequence, the NBDs are conserved with respect to structure and function. Interestingly, the NBD of TAP1 contains mutations at amino acid positions that have been proposed to be essential for catalytic activity. Instead of a glutamate, proposed to act as a general base, TAP1 contains an aspartate and a glutamine instead of the conserved histidine, which has been suggested to act as the linchpin. We used this degeneration to evaluate the individual contribution of these two amino acids to the ATPase activity of the engineered TAP1-NBD mutants. Based on our results a catalytic hierarchy of these two fundamental amino acids in ATP hydrolysis of the mutated TAP1 motor domain was deduced.

ATP-binding cassette (ABC)[3]-transporters form a large superfamily of primary transmembrane proteins (1), which ultimately use the energy of ATP hydrolysis to translocate their substrate or allocrite (2), the term we prefer to distinguish the transported substrate from ATP. Found in all three kingdoms of life, ABC-transporters contain certain sequence motifs such as the Walker A and B motifs, the C-loop (ABC signature motif), and the D-loop (3, 4). These sequences serve as diagnostic tools to identify ABC-transporters. Furthermore, all members of this family show a modular architecture composed of two nucleotide-binding domains (NBDs), which contain all the conserved sequence motifs, and two transmembrane domains (TMDs). In archea and eubacteria, these four modules are generally encoded on separate genes, whereas they are fused on a single polypeptide chain ("full-size" transporter) in eukarya. Additionally, fusions of one NBD and one TMD, which are called "half-size" transporters, are found in all organisms. The functional unit of these systems would be a homo- or heterodimer of two half-size transporters. Examples of the latter are hemolysin B (HlyB) from *Escherichia coli* (5) and the human transporter associated with antigen processing (TAP) (6).

Human TAP, located in the membrane of the endoplasmic reticulum (ER), is a key component of major histocompatibility complex class I-mediated adaptive immunity (7). The functional TAP complex is a heterodimer composed of TAP1 and TAP2, both of which comprise a TMD-NBD fusion. It is now firmly established that the allocrites of TAP, antigenic peptides, which are generated in the cytosol by proteasomal degradation (8, 9), are transported in an ATP-dependent manner across the ER membrane for subsequent loading of major histocompatibility complex class I molecules (10). After passing the ER quality control, peptide-major histocompatibility complex class I complexes travel to the cell surface and present their antigenic cargo to $CD8^+$ T-lymphocytes. Although both NBDs are capable of binding and hydrolyzing ATP (11–14), it was demonstrated that the two NBDs of the TAP complex behave nonequivalent in functional terms (11–13, 15–17). Thus, one could envision a regulatory function of one NBD, whereas the other NBD of the TAP complex actually fuels peptide translocation. Such an asymmetric behavior of the NBDs with respect to ATP hydrolysis is reminiscent of CFTR (18) or MRP1 (19–21). Here, experimental data suggest that the N-terminal NBD serves as a regulatory domain, whereas the C-terminal NBD provides the energy necessary for allocrite translocation via ATP hydrolysis.

Crystal structures of full-length ABC-transporters (22–25) and isolated NBDs (for recent reviews see Refs. 3, 26, and 27) have provided many valuable insights into the function of the ABC cassettes. In the ATP-bound state, NBDs form a composite dimer (28–30). Here, ATP is sandwiched between the Walker A motif of one monomer and the C-loop of the other monomer. This in combination with biochemical data (see, *e.g.* Refs. 31–33) has led to the identification of certain key amino acids important for ATP binding and hydrolysis. For instance, it was shown that a glutamate adjacent to the Walker B motif is important for ATP hydrolysis, because mutation to a glutamine abolished ATPase activity (32). It was therefore postulated that this glutamate acts as "general base" (34, 35), *i.e.* abstracts a

* This work was supported by the Deutsche Forschungsgemeinschaft (Emmy Noether program, Grant Schm1279/2-3 to L. S.). The costs of publication of this article were defrayed in part by the payment of page charges. This article must therefore be hereby marked "*advertisement*" in accordance with 18 U.S.C. Section 1734 solely to indicate this fact.

[1] Present address: CellGenix GmbH, Am Flughafen 16, 79108 Freiburg, Germany.

[2] To whom correspondence should be addressed. Tel.: 49(0)221-81-10773; Fax: 49(0)211-81-15310; E-mail: lutz.schmitt@uni-duesseldorf.de.

[3] The abbreviations used are: ABC, ATP-binding cassette; CFTR, cystic fibrosis transmembrane conductance regulator; MRP, multidrug resistance-related protein; NBD, nucleotide-binding domain; TAP, transporter associated with antigen processing; TMD, transmembrane domain; TNP-ADP, 2′,3′-*O*-(2,4,6-trinitrophenylcyclohexadienylidene)adenosine ditriphosphate; ER, endoplasmic reticulum; HlyB, hemolysin B.

proton from the attacking water molecule in the rate-limiting step of hydrolysis. Results from full-length ABC-transporters and isolated NBDs supported this idea (see, *e.g.* Refs. 34 and 36). However, more and more results have challenged the role of the conserved glutamate as a catalytic base (37–42). In the case of the maltose and histidine permeases, mutation of a histidine located in the H-loop sequence abolished ATPase activity and/or allocrite translocation (31, 33, 43). For the NBD of HlyB, a mutation of the corresponding histidine to alanine (H662A) eliminated ATPase activity as well, whereas residual ATPase activity was detected in the glutamate to glutamine mutant (E631Q) (30). These data, which were supported by the crystal structure of the HlyB-NBD H662A mutant with bound ATP/Mg^{2+}, led to the proposal of a different model (30). Here, the glutamate and the histidine form a catalytic dyad, with the glutamate stabilizing a productive conformation of the histidine, which stabilizes the transition state of ATP hydrolysis. Furthermore, according to this "linchpin" model, ATP hydrolysis does not follow general base catalysis, but rather "substrate-assisted catalysis" as proposed for the $p21^{ras}$ oncogene (44).

So far, crystal structures of dimeric ABC cassettes with bound ATP were solved only for homodimeric NBDs (28–30). However, many ABC-transporters from higher organisms contain two different ABC cassettes. In the human TAP complex, the ATP-induced NBD-dimer is composed of the motor domains of TAP1 and TAP2. Sequence comparison of these NBDs and the two NBDs of human CFTR and human MRP1 (Fig. 1) reveal important amino acid replacements for catalytically relevant residues. First, TAP2 and the C-terminal NBDs of CFTR and MRP1 do not contain the essential second glycine of the C-loop, which, according to the crystal structures of ATP-bound, dimeric ABC cassettes, interacts with the γ-phosphate moiety of the bound ATP. Second, the glutamate, the proposed catalytic carboxylate, adjacent to the Walker B motif, is replaced by an aspartate in TAP1 and by a serine in the N-terminal NBD of CFTR. Third, the essential histidine of the H-loop, proposed to act as the linchpin, is not present in TAP1 and the N-terminal NBD of CFTR. In light of the ATP-bound dimer of NBDs, this arrangement would generate one ATP-binding site with drastically reduced or even no ATPase activity (Walker A motif of monomer 1 and C-loop of monomer 2 but no glutamate and no histidine) and one site capable of hydrolyzing ATP (Walker A motif, glutamate, and the histidine of the H-loop of monomer 2 and the C-loop of monomer 1). Such degeneration would explain the asymmetric behavior of these (11–21, 45) and other ABC-transporters on a molecular level. More important, however, is the fact that the deviation of the primary structure in the TAP1-NBD with respect to the glutamate and histidine provides a perfectly suited model system to analyze the function of these two essential amino acids during the catalytic cycle of an NBD on a molecular level and their contribution to ATPase activity.

Here, we report mutational studies of the isolated ABC cassette of human TAP1. The aspartate at position 668 was mutated to glutamate (D668E), and at position 701 the conserved histidine was introduced (Q701H). Additionally, the double mutant was generated (D668E/Q701H). The double mutant, representing the canonical sequence of ABC cassettes, displayed basal ATPase activity. More important, however, is the fact that the single mutants (D668E and Q701H) behaved differently. Although the D668E mutant like the wild-type enzyme did not show ATPase activity, reintroduction of the histidine in the absence of the glutamate (Q701H) resulted in an ATPase-active enzyme, although at a reduced level compared with the double mutant (D668E/Q701H). Thus, the results indicate different functional roles of these two conserved amino acids during the catalytic cycle and clearly support the importance of the H-loop histidine for ATPase activity suggesting that a catalytic dyad composed of the glutamate and the histidine is created in the isolated ABC cassette of TAP1.

MATERIALS AND METHODS

Heterologous Expression of TAP1-NBD and Mutants in E. coli—The C-terminal domain (amino acids 489–748) of TAP1 was amplified by PCR on cDNA coding for TAP1 using the primers: 5′-GGAATTCCATATGGGCAGCAGCCATCACCATCACCATCACCCACCCAGTGGTCTGTTGACTCCC-3′ and 5′-ATATATAAAGCTTATCATTCTGGAGCATCTGCAGGAGCCTG-3′. The 5′-extensions encoded NdeI and HindIII restriction sites, respectively, and an N-terminal hexahistidine tag. The resulting PCR product was cloned into the NdeI and HindIII sites of the expression vector pET21a+ (Novagen). Amino acid substitutions (in single and double) were introduced by site-directed mutagenesis one amino acid downstream of the Walker B motif (D668E, GAT → GAA) and at the position of the conserved histidine (Q710H, CAA → CAC). Thus, four plasmids pET-NBD(wt), pET-NBD(D668E), pET-NBD(Q710H), and pET-NBD(D668E/Q710H), were generated. For expression, the *E. coli* strain BL21(DE3) (Novagen) was transformed with the plasmids and grown in LB medium with 100 μg/ml ampicillin at 30 °C. At an A_{600} of 0.5 the cells were induced with 1 mM isopropyl-β-D-thiogalactopyranoside and harvested after 3 h by centrifugation (4000 × *g*, 15 min, 4 °C).

Purification of TAP1-NBD—All purification steps were performed at 4 °C. The cell pellet of a 2-liter culture was resuspended in 30 ml of pre-chilled buffer A (20 mM sodium phosphate, 50 mM NaCl, 10 mM imidazole, 15% w/v glycerol, pH 8) supplemented with 1 mg/ml lysozyme and 0.1 mg/ml deoxyribonuclease I from bovine pancreas (Fluka). After 15-min incubation, cells were broken by cell rupture treatment (2.7 kbar, Basic Z Model, Constant Systems). Unbroken cells and cell debris were removed by centrifugation (16,000 × *g*, 30 min, 4 °C). The supernatant corresponding to the cytosolic fraction was loaded onto a Zn^{2+}/iminodiacetic acid column (5-ml volume, GE Healthcare, Freiberg, Germany) pre-equilibrated with buffer A. Nonspecifically bound proteins were eluted employing a step gradient of 6 column volumes of buffer A and 6 column volumes of buffer A supplemented with 25 mM imidazole. All TAP1-NBD variants were eluted with 90 mM imidazole in buffer A. The TAP1-NBD containing fractions were immediately adjusted to 20 mM dithiothreitol, pooled, and concentrated by ultrafiltration (Amicon Ultraspin concentrators, 10 kDa, Millipore). The soluble TAP1-NBD was further purified and separated from aggregates on a Superdex 200 HR 26/60 column (320-ml bed volume, GE Healthcare) equilibrated with

buffer B (20 mM Tris, 50 mM NaCl, 15% w/v glycerol, pH 8). The NBD eluted with an apparent molecular weight of 29 kDa corresponding to the size of the monomer. Fractions were stored on ice at a concentration of ~1 mg/ml. Wild-type and mutant proteins were purified to >99% homogeneity by this two-step procedure as assessed by Coomassie-stained SDS-PAGE (15%).

ATPase Activity Assay—ATPase activity was analyzed as described previously (46) with the following modifications: the activity assay of TAP1-NBD (1 mg/ml) was performed in buffer B at 30 °C. Time- and pH-dependent ATPase activity was assayed in the presence of 2 mM ATP and 5 mM $MgCl_2$. The reaction was stopped with 40 mN H_2SO_4, and the amount of liberated P_i was determined by a colorimetric assay, using Na_2HPO_4 as standard.

TNP-AXP Binding Studies—To assess the binding affinity of ATP and ADP to the TAP1-NBD and their mutant versions, we used the fluorescent nucleotide analogues TNP-ATP and TNP-ADP (Molecular Probes) . Binding studies were generally performed as described previously (47). Fluorescence of TNP nucleotides was monitored at 540 nm using a Fluorolog (Horiba, Edison, NJ). The excitation wavelength was set at 409 nm, the slit width at 4 nm, and the temperature was maintained at 20 ± 1 °C. All experiments were performed in buffer B supplemented with the appropriate $MgCl_2$ concentration in a total volume of 1400 μl.

Upon binding of TNP-A*X*P (*X* = M, D, or T) to the TAP1-NBD, the fluorescence intensity of TNP-A*X*P enhances severalfold. The absolute magnitude depends on the specific protein environment within the nucleotide-binding pocket and was introduced as a fitting parameter (see below). The fluorescence intensity of TNP-A*X*P in buffer is low in the absence of TAP1-NBD and can be described by Equation 1, taking inner filter effects into account (48, 49). The fluorescence constants Q_1 and Q_2 in buffer B (with and without 5 mM $MgCl_2$) were determined in the absence of protein by stepwise addition of TNP-A*X*P from a 1 mM stock solution to assay buffer. The maximal change of volume was kept below 4% (v/v), and the fluorescence intensity was corrected for dilution and background fluorescence in the absence of any TNP-A*X*P. All data represent the average value of at least two independent measurements.

$$F_{\text{buffer}} = Q_1 L_0 + Q_2 L_0^2 \qquad \text{(Eq. 1)}$$

Here, Q_1 and Q_2 denote the specific fluorescence constants of TNP-A*X*P, and L_0 is the concentration of TNP-A*X*P.

The TAP1-NBD and their mutants were diluted into buffer B supplemented with 5 mM $MgCl_2$ and titrated with TNP-A*X*P as described above at a concentration of 150 μg/ml. The dissociation constant (K_D) of the TAP1-NBD/TNP-A*X*P complexes was determined according to Equation 2,

$$F = Q_1 L_0 + Q_2 L_1^2 + F_{\max}(A - \sqrt{A^2 - 4L_0 NP_0}) \qquad \text{(Eq. 2)}$$

$$A = K_D + L_0 + NP_0 \qquad \text{(Eq. 3)}$$

where Q_1 and Q_2 denote specific fluorescence constants, which were determined independently (see above), and $F_{\max}$ is the maximal fluorescence due to TNP-A*X*P binding to the TAP1-NBD. L_0 and P_0 are the total concentration of TNP-A*X*P and TAP1-NBD, respectively. K_{D_L} is the dissociation constant of the TAP1-NBD/TNP-A*X*P complex. *F* defines the measured fluorescence.

Competitive Binding Studies of TAP1-NBD/TNP-ADP Complexes—The TAP1-NBD (150 μg/ml) was preincubated with 10 μM TNP-ADP for 2 min at 20 (±1) °C. At this concentration, ATP-induced dimerization is negligible (see below). Subsequently, A*X*P (*X* = T, D, or M) was added in a stepwise fashion from a 2 μM, 20 μM, 200 μM, 2 mM, 20 mM, 200 mM, and 500 mM stock solution at pH 8 to a final ATP concentration of maximal 20 mM. The maximal dilution was <4% (v/v). The fluorescence data were corrected for background fluorescence, normalized, and analyzed according to Equation 4 (47),

$$\frac{F_{PL_N,AXP}}{F_{PL_N}} = \frac{A + AXP_0 \frac{K_{D_L}}{K_{D_{AXP}}} - \sqrt{\left(A + AXP_0 \frac{K_{D_L}}{K_{D_{AXP}}}\right)^2 - 4NP_0L_0}}{A - \sqrt{A^2 - 4NP_0L_0}} \qquad \text{(Eq. 4)}$$

where $F_{P_L,AXP}/F_{P_L}$ defines the normalized fluorescence at different A*X*P concentrations (A*X*P, *X* = T, D, or M). K_{D_L} is the dissociation constant of the TAP1-NBD/TNP-ADP complex in the presence or absence of 5 mM $MgCl_2$ and was determined independently (see above). L_0 and P_0 are the total concentrations of TNP-ADP and TAP1-NBD, respectively. K_D, a*x*p is the dissociation constant of TAP1-NBD/A*X*P complexes, and *A* has been defined in Equation 3. K_D values of TAP1-NBD/A*X*P complexes are the average value of at least two independent titration experiments.

Molecular Modeling—The molecular model of the TAP1-NBD/TAP2-NBD heterodimer with bound ATP/Mg^{2+} was generated based on the crystal structure of the HlyB-NBD H662A dimer in complex with ATP/Mg^{2+} (pdb entry 1XEF). After sequence alignment using the ClustalW web interface (www.ebi.ac.uk/clustalw/) employing the sequences shown in Fig. 1, the SWISS model web server (swissmodel.expasy.org/) was used following the outlines of the authors without manual interference.

RESULTS AND DISCUSSIONS

Sequence alignments of the ABC cassettes of human TAP1 and TAP2 with both NBDs of human CFTR and human MRP1, respectively, and bacterial NBDs, for which crystal structures of the dimeric, ATP-bound state were reported (28–30), are shown in Fig. 1. The alignment revealed a somewhat regular pattern of important deviations from the classic primary structure in the human motor domains. In human TAP1 and in the N-terminal motor domains of CFTR and MRP1, the conserved glutamate, the putative catalytic base, is replaced by an aspartate (Asp-668 in TAP1, Asp-573 in CFTR, and Asp-793 in MRP1). In addition, the histidine of the H-loop, the putative linchpin, is replaced by a glutamine in TAP1 (Gln-701) and a serine in CFTR (Ser-604), whereas a histidine is present in MRP1 (His-827). This situation is reminiscent of the recently described bacterial multidrug tranporter LmrCD from *Lactococcus lactis*. LmrC shows the above indicated deviations from the canonical sequences and in terms of primary structure

	Walker A / Q-loop	C-loop	Walker B / D-loop	H-loop
TAP1	---GPNGSGKST---Q----	LSGGQ-	VLILDDATSALD-	-Q---
TAP2	---GPNGSGKST---Q----	LAAGQ-	VLILDEATSALD-	-H---
CFTR(N)	---GSTGAGKTS---Q----	LSGGQ-	LYLLDSPFGYLD-	-S---
CFTR(C)	---GRTGSGKST---Q----	LSHGH-	ILLLDEPSAHLD-	-H---
MRP1(N)	---GQVGCGKSS---Q----	LSGGQ-	IYLFDDPLSAVD-	-H---
MRP1(C)	---GRTGAGKSS---Q----	LSVGQ-	ILVLDEATAAVD-	-H---
MalK	---GPSGCGKST---Q----	LSGGQ-	VFLLDEPLSNLD-	-H---
MJ0796	---GPSGSGKST---Q----	LSGGQ-	IILADEPTGALD-	-H---
HlyB	---GRSGSGKST---Q----	LSGGQ-	ILIFDEATSALD-	-H---

FIGURE 1. **Sequence alignment of selected ABC domains of ABC-transporters and those NBDs, for which crystal structures of the dimeric, ATP-bound state have been reported (28–30).** For simplicity, only the conserved motifs are shown. The spacing between the individual motifs reflects the number of amino acids inserted between two adjacent motifs. Evident is the degeneration of the motor domain of TAP1 and the N-terminal NBDs of CFTR and MRP1 with respect to the "glutamate" residue C-terminally to the Walker B motif and the conserved "histidine" of the H-loop. Note that in the sequence of MJ0796, the Glu of the wild-type protein was substituted to a Gln (E171Q mutant) to obtain crystals, which could be used for the structure determination of the ATP-bound sandwich dimer (29).

would correspond to TAP1, whereas LmrD would correspond to TAP2 (50). Furthermore, the C-loop of TAP2 and the C-terminal ABC cassettes of CFTR and MRP1 do not contain the consensus sequence (LSGGQ). Here, LAAGQ replaces the LSGGQ sequence in TAP2, LSHGQ in CFTR, and LSVGQ in MRP1. Thus, the absence of the two catalytically important residues (Glu and His) together with the deviation of the canonical C-loop sequence of TAP2 will impose certain restrains on the architecture of both ATP-binding sites, and it was indeed shown that the asymmetric C-loop sequences of TAP have a strong impact on peptide transport efficiencies *in vitro* (16).

Currently, three crystal structures of dimeric motor domains with bound ATP have been solved (28–30). Here, the ABC cassette of the *E. coli* transporter HlyB shows the highest degree of sequence identity with the motor domains of TAP (39% identity with TAP1 and 43% with TAP2). The similarity is 73% (TAP1) and 76% (TAP2). In contrast, sequence identity is reduced to 25% (TAP1 and TAP2) in the case of MJ0796 and to 28% (TAP1) and 29% (TAP2) in the case of MalK. Therefore, a structural model of the ATP-bound composite heterodimer of the NBDs of TAP1 and TAP2 was generated using the crystal structure of the ATP/Mg^{2+}-bound dimer of HlyB (for further details see "Materials and Methods"). The obtained structural model is shown in Fig. 2. As already expected from the sequence, the ATP-binding sites are asymmetric. Site A is composed of the Walker A and B motifs, the putative catalytic carboxylate (Glu-632), and the putative linchpin (His-661) of TAP2 and the C-loop of TAP1, which contains the canonical sequence (LSGGQ). In contrast, site B includes the Walker A and B motifs of TAP1 and the C-loop of TAP2, which is degenerated (LAAGQ). In addition, both, the glutamate and histidine are replaced in TAP1 by an aspartate (Asp-668) and a glutamine (Gln-701), respectively. Thus, site A reveals a classic arrangement of catalytically relevant amino acids in a productive fashion, whereas the second site (site B) is corrupted. The C-loop, which is essential for forming the composite dimer architecture, and the glutamate and the histidine, both of which have been proposed to be the catalytically important residue during

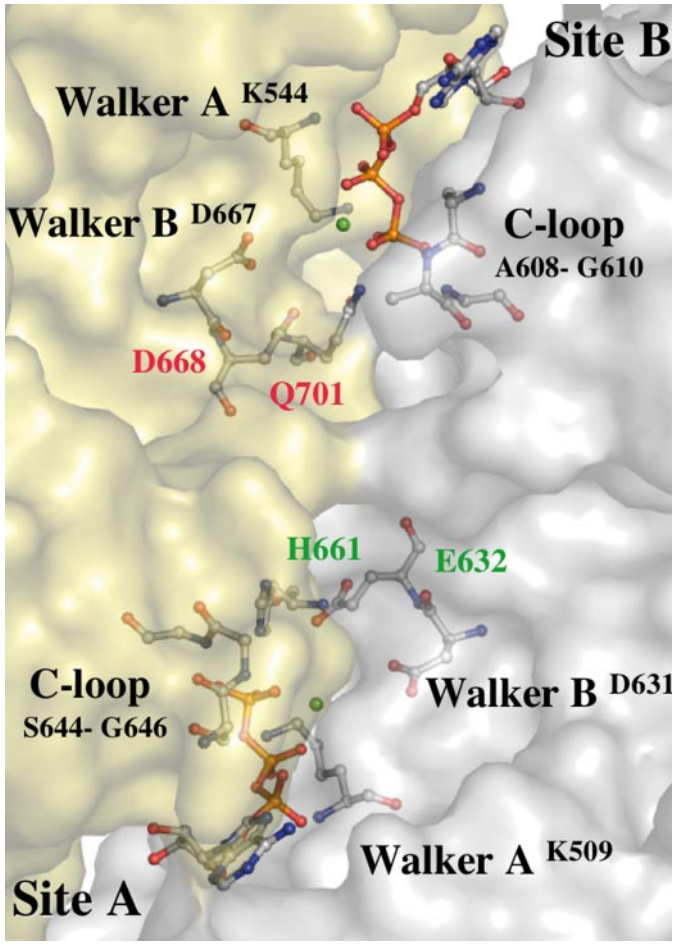

FIGURE 2. **Structural model of the TAP1-NBD/TAP2-NBD dimer with bound ATP/Mg^{2+}.** The model was generated based on the ATP/Mg^{2+} composite dimer of HlyB (pdb entry 1XEF) using the SWISS model web server (swissmodel.expasy.org). TAP1-NBD and TAP2-NBD are shown as *transparent solids* in *yellow* and *gray*, respectively. Bound ATP is shown in *ball-and-stick representation* and Mg^{2+} as *green spheres*. Catalytic essential residues of the two ATP-binding sites are highlighted in *ball-and-stick representation* and *labeled*. For simplicity, only the lysines of the Walker A and the aspartates of the Walker B motifs and a reduced C-loop are shown. The degenerated and functionally important residues Asp-668 and Q701 of TAP1 are indicated in *red*, whereas the corresponding residues in TAP2 are specified in *green* (Glu-632, the putative catalytic base, and His-661, the linchpin). For further details please see text.

ATP hydrolysis (30, 32, 34, 41), are exchanged to non-productive amino acids. However, this sequence and structure degeneration of the ABC cassette of TAP1 also opens up the possibility to analyze the role of these two amino acids during catalysis directly and to distinguish the proposals, which are diametrically opposed.

Accordingly, the ABC cassettes of wild-type TAP, the single mutants D668E and Q701H, and the double mutant D668E/Q701H were generated and purified following the procedure of Gaudet and Wiley (51) with modifications as outlined under "Materials and Methods." All proteins were purified by a two-step procedure to near homogeneity with a purity >99% (Fig. 3). Based on gel-filtration experiments (data not shown), all proteins eluted as monomeric species with an apparent molecular mass of 29 kDa. With this set of proteins, the individual influence of the glutamate (D668E mutant), proposed to act as general base, and the histidine (Q701H mutant), proposed to

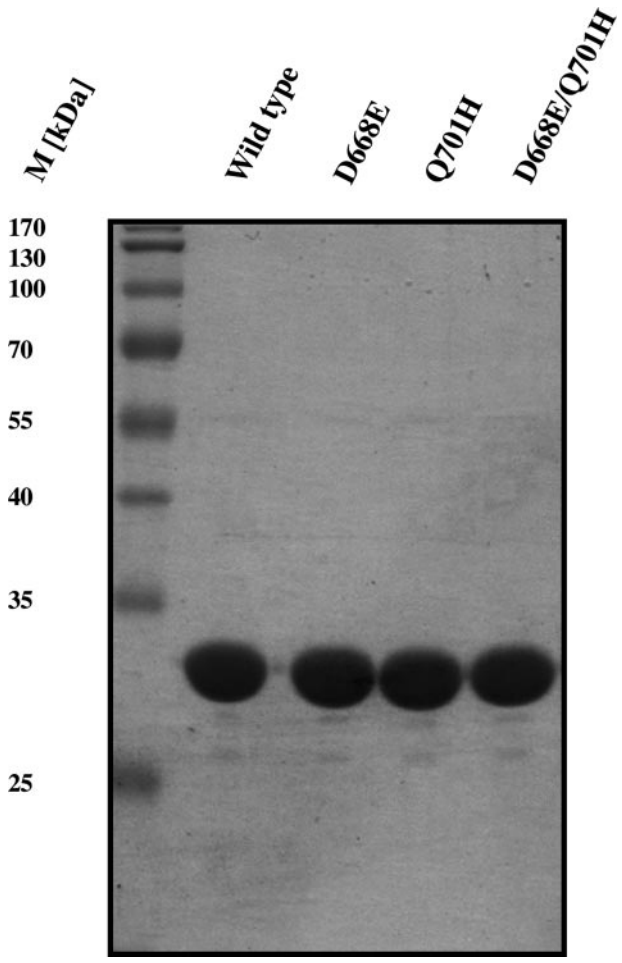

FIGURE 3. **Coomassie-stained SDS-PAGE (15%) of wild-type TAP1-NBD and the three mutants used in this study after the final gel-filtration step.** The molecular masses of the marker proteins are given to the *left*.

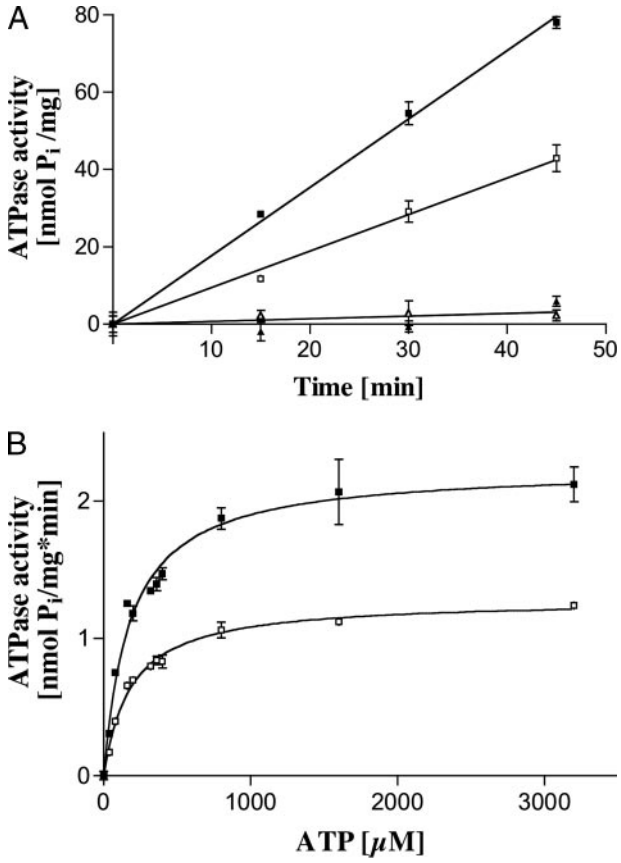

FIGURE 4. *A*, time-dependent ATPase activity of wild-type (*filled triangles*) TAP1-NBD and the D668E (*open triangles*), Q701H (*open squares*), and D668E/Q701H (*filled squares*) mutants. Analysis was performed at 30 ± 2 °C at a protein concentration of 1 mg ml^{-1} (30 μM) and pH 8.0. Data points represent the average of two independent experiments with the standard deviation reported as errors. *B*, ATP concentration-dependent ATPase activity of the Q701H (*open squares*) and D668E/Q701H (*filled squares*) mutants at 30 ± 2 °C at a protein concentration of 1 mg ml^{-1} (30 μM) and pH 8.0. Data points represent the average of two independent experiments with the standard deviation reported as errors and were analyzed according to the Michaelis-Menten equation. Kinetic parameters were determined to be: K_m = 174 ± 17 μM (Q701H) and 180 ± 21 μM (D668E/Q701H) and v_{max} = 1.26 ± 0.04 nmol of P_i/min·mg (Q701H) and 2.24 ± 0.08 nmol of P_i/min·mg (D668E/Q701H). All experiments were performed at a concentration of ATP of 2 mM.

act as linchpin, as well as a potential synergistic effect of both mutations (D668E/Q701H) could be directly analyzed by studying the ATPase activity of the corresponding proteins in solution.

At a protein concentration of 1 mg/ml, the wild-type TAP1-NBD displayed no significant ATPase activity (Fig. 4*A*, *filled triangles*). In clear contrast, the double mutant (D668E/Q701H) showed ATPase activity (Fig. 4*A*, *filled squares*). Because this mutant contains both residues that have been suggested to be essential for activity, the result of this mutant was to some degree expected and serves as a positive control in our mutational studies. More important are the results obtained for the single mutants. The single glutamate mutant (D668E) showed no significant ATPase activity (Fig. 4*A*, *open triangles*). On the other hand, engineering a single mutant at position 701 of TAP1 (Q701H), which corresponds to the H-loop of ABC cassettes, generated an ATPase-active NBD (Fig. 4*A*, *open squares*). Evidently, replacement of both canonical amino acids at position 668 and 701 of TAP1 induced the highest rate of ATPase activity, but already the histidine at position of 701 is essential and sufficient for a substantial generation of ATPase activity. Using the concept of Mildvan (52), the non-additive influence of the single mutants on the ATPase activity of the double mutant suggests some sort of cooperative interaction between the glutamate and the histidine (see below). To further evaluate the active forms of TAP1-NBD, kinetic parameters of the D668E/Q701H and the Q701H mutants were determined (Fig. 4*B*). Both proteins followed Michaelis-Menten kinetics with K_m values of 180 ± 21 μM (D668E/Q701H) and 183 ± 15 μM (Q701H) and v_{max} values of 2.24 ± 0.08 nmol of P_i/mg·min, k_{cat} = 0.06 ATP/min (D668E/Q701H) and 1.28 ± 0.04 nmol of P_i/mg·min, k_{cat} = 0.03 ATP/min (Q701H) at pH 8. These values are comparable to other isolated NBDs ((53) and references therein) but much lower than the basal ATPase activity of intact transporters, which ranges from 1.5 ATP/min (PrtD (54)) to 4.5 ATP/s (P-glycoprotein (38)). In case of isolated NBDs, the reported k_{cat} values range from 5×10^{-5} ATP s^{-1} (MRP1-NBD (55)) to 26 ATP min^{-1} (HisP (56)). Despite these enormous differences in activity, crystal structures of NBDs, including that of MRP1-NBD (57), provide no indication that major changes in the molecular mechanism of ATP hydrolysis occur regardless of the turnover number. Thus, from a mechanistic point of view, these results demonstrate that the glutamate in

TABLE 1

Equilibrium binding constants of nucleotides to wild-type NBD and the D668E, Q701H, and D668E/Q701H mutants in the presence or absence of the 5 mM Mg^{2+} at 20 ± 1 °C

Affinity constants were determined from competition experiments as described under "Materials and Methods." Values represent the average of at least two independent experiments.

System	Nucleotide	Cofactor	K_D
			μM
Wild type	ATP	+	22.9 ± 1.3
		−	400.6 ± 21.7
	ADP	+	3.3 ± 0.4
		−	121.9 ± 27.6
	AMP	+	>20,000
		−	>20,000
D668E	ATP	+	8.4 ± 0.3
		−	424.1 ± 21.8
	ADP	+	1.6 ± 0.1
		−	32.6 ± 5.4
	AMP	+	>20,000
		−	>20,000
Q701H	ATP	+	2.7 ± 0.4
		−	367 ± 34.9
	ADP	+	0.4 ± 0.1
		−	99.1 ± 9.9
	AMP	+	>20,000
		−	>20,000
D668E/Q701H	ATP	+	17.2 ± 2.2
		−	459.9 ± 38.8
	ADP	+	2.3 ± 0.2
		−	28.8 ± 1.6
	AMP	+	>20,000
		−	>20,000

the double mutant is responsible for a higher efficiency of substrate hydrolysis, whereas the K_m values of the Q701H and the double mutant are identical within experimental error. This might suggest for example that the glutamate is not acting as a catalytic residue but rather as a residue imposing a structural effect on the catalytically relevant and active histidine. The observed differences between wild-type and Q701H might also imply some sort of distance-dependent interaction, because an aspartate and the engineered glutamate (D668E and double mutant) differ by only one methylene unit.

The results of the ATPase measurements suggested a hierarchy between the glutamate and histidine in ATP hydrolysis. However, one could also explain the observed outcome by a drastic change in nucleotide affinity, *i.e.* that the wild-type and the D668E mutant possess an extremely low affinity toward ATP or that the affinity of these two enzymes toward ADP is extremely high (other possibilities are discussed below). In such a scenario, introduction of a histidine at position 701 might alter this behavior, which would render the Q701H and the double mutant susceptible for ATP binding and subsequent hydrolysis. Such a hypothetical change in nucleotide affinity is supported by the crystal structure of the TAP1-NBD (51). Although crystallization trials were performed in the presence of ATP/Mg^{2+}, ADP/Mg^{2+} was bound to the protein in the crystal. To distinguish these two scenarios, we determined the affinities of all four enzymes toward ATP, ADP, and AMP in the presence or absence of the cofactor Mg^{2+} (Table 1) by competition experiments using TNP-labeled nucleotides (47). As expected, the isolated ABC cassettes did not show any affinity to AMP regardless of the presence or absence of Mg^{2+}. In contrast, wild-type, both single mutants, and the double mutant enzymes bound ADP and ATP. In all cases, the affinity for ADP was higher than for ATP, a situation reminiscent of the HlyB-NBD (41). However, in striking contrast to the HlyB-NBD, the cofactor modulated the equilibrium binding affinities. In the presence of Mg^{2+}, the affinity for ADP was roughly 6-fold higher than for ATP, whereas the difference in affinity varied between 4- and 15-fold in the absence of Mg^{2+}. Even more pronounced is the Mg^{2+} modulation for the same nucleotide. For example, the cofactor increased the ATP affinity 18-fold for the wild-type enzyme, 50-fold for the D668E mutant, 120-fold for the Q701H mutant, and 27-fold for the double mutant. This striking increase implies a conformational change within the motor domain upon cofactor binding, a situation different to HlyB-NBD (41) but qualitatively similar to P-glycoprotein (58). For the purpose of our investigations, however, relative changes in nucleotide affinities upon introduction of different mutations are more important. In the case of ATP/Mg^{2+}, the affinity of the protein increases from wild-type to D668E and to Q701H, but it decreases again for the double mutant, which possessed an affinity close to that of the wild-type protein. In the absence of Mg^{2+}, hardly any changes in affinity for the four enzymes are detectable. The same behavior is observed for ADP in the presence or absence of the cofactor. Thus, changes in steady-state affinities of the nucleotides cannot account for the observed differences in ATPase activity (which was assayed in the presence of 2 mM ATP), and implementation of a histidine at position 701 of TAP1-NBD is sufficient and the only requirement to generate an enzyme capable of hydrolyzing ATP. Furthermore, the presence of glutamate/histidine (D668E/Q701H) reduces the affinity for ATP compared with the aspartate/histidine (Q701H) mutant. This trend is reversed in the absence of the histidine (wild type and D668E) suggesting some kind of differential interaction between the carboxylates and the histidine. Interestingly, similar changes in affinity for ATP were seen in MRP1 (42) upon replacing the naturally occurring aspartate with glutamate.

It is now commonly accepted that ATP induces dimerization of isolated ABC cassettes and that the dimer is the catalytically relevant species during ATP hydrolysis (32, 36, 41, 59). In archea and eubacteria, both NBDs are in general catalytically active. In contrast, in eukarya many ABC-transporters according to their primary structure form one active and one inactive or strongly impaired ATP-binding site. Examples of the latter are the TAP heterodimer, CFTR, or MRP1. This "degeneration" of the CFTR-NBDs has led to a proposal, in which one of the two ATP-binding sites undergoes frequent cycles of ATP hydrolysis and binding, while the other one acts as a re-setting or controlling unit (60, 61). Assuming that the same model is operational in TAP, site A would be catalytically active and site B would be inactive (Fig. 2). From a mechanistic point of view, it is important to determine which amino acid mutants render site B, *i.e.* the aspartate/glutamate or the glutamine/histidine exchange, inactive. However, to address this question, a heterodimeric architecture necessitates simplification. Therefore, we rationalized that an artificial TAP1-NBD system without interference from the TAP2-NBD would provide the proper model system to study these questions under defined conditions. Obviously, the issue of whether the detectable ATPase activity of the Q701H and the D668E/Q701H mutants of

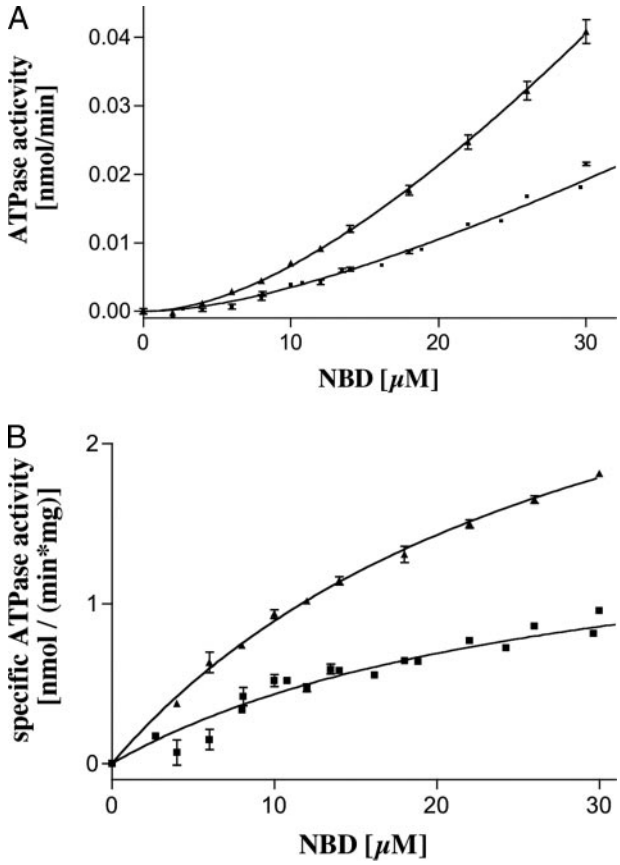

FIGURE 5. *A*, protein concentration-dependent ATPase activity of the D668E/Q701H (*filled triangles*) and the Q701H (*filled squares*) mutant at 30 ± 1 °C and pH 7.2. *B*, protein concentration-dependent and -specific ATPase of the D668E/Q701H (*filled triangles*) and the Q701H (*filled squares*) mutant at 30 ± 1 °C and pH 7.2. Data points represent the average of two independent experiments.

TAP1-NBD arises from the monomeric or the dimeric species of the ABC cassette is of paramount importance for such investigations. To distinguish monomer- and dimer-derived ATPase activity of the motor domain, we consequently analyzed the protein concentration-dependent ATPase activity of the double mutant (Fig. 5*A*) at pH 7.2. For a monomeric protein, which hydrolyzes ATP, a linear dependence of activity is expected in such a representation (56). Because this is clearly not the case, ATP hydrolysis derives from a higher oligomeric species. To determine the apparent oligomerization constant K_D^{app}, we plotted the *specific* ATPase activity *versus* protein concentration (Fig. 5*B*). Here, the observed saturation and hyperbolic shape of the curve indicate that a higher oligomeric species, likely the dimer, is catalytically relevant, because a constant value irrespective of protein concentration would be expected if a monomer was active. A quantitative analysis revealed a K_D^{app} of 30 ± 2 μM for the double mutant and a K_D^{app} of 28 ± 6 μM for the Q701H mutant. However, this analysis is not intended to provide an exact value for the dimerization constant of the TAP1-NBD, because the protein concentrations, which can be employed, are not high enough to derive reliable affinities from these data. Nevertheless, these data demonstrate that a low affinity oligomerization is functionally indispensable for activity and furthermore explains why detection of the dimeric ATP-bound species was not possible by other techniques such as size exclusion chromatography (data not shown).

Based on the data obtained for other isolated motor domains (32, 36, 41, 59), it is conceivable to assume that, also in the TAP1 double mutant, a dimer is the catalytically active species. However, as pointed out above, the derived apparent dimerization constant rather serves as an estimate and not as a quantitative value as the K_D^{app} determined for HlyB-NBD (41), OpuAA (47), or Mdl1p-NBD (36), because of the abovementioned reasons. Clearly, the complex enzyme kinetics obtained for HlyB-NBD (41) and as explained here for TAP1-NBD also imply that the concentration of the NBD dramatically influences the rate-limiting step of the ATPase cycle. As pointed out, at low protein concentrations, the probability of dimer formation becomes limiting, whereas at high concentrations (above K_D^{app}), the dimerization step will not influence the catalytic efficiency anymore. Thus, dimerization is not the rate-limiting step in a full-length ABC-transporter due the high local concentration of the NBDs. This interpretation might also help to clarify recent discrepancies concerning the rate-limiting step of ATP hydrolysis in isolated ABC cassettes (30, 62).

The mutational studies within the ABC cassette of TAP1 allowed us to distinguish the influence of the canonical glutamate (putative catalytic base) and the histidine (putative linchpin). According to our interpretation, the glutamate is not directly involved in catalysis, whereas the histidine is of prime importance. However, the presence of both amino acids, the glutamate and the histidine, increased the ATPase activity by a factor of two at pH 8.0 when compared with the histidine mutation. To analyze this behavior in more detail and to exclude other possible models explaining the observed differences, the pH dependence of the Q701H and the D668E/Q701H mutants was recorded (Fig. 6). The Q701H displayed a sigmoidal-like curve, whereas the double mutant activity profile was bell-shaped. The increase of activity of both enzymes around pH 5.0 is qualitatively identical. This implies the same arrangement of catalytic amino acids. However, the activity of the Q701H remained on a constant level at pH values larger than 7.0 (Fig. 6*A*), whereas the double mutant showed a decrease in activity (Fig. 6*B*). The only difference between these two mutants occurs at position 668, aspartate (in the Q701H mutant) or glutamate (in the double mutant). Therefore, one can pinpoint the origin of this altered pH dependence to the only difference between an aspartate and a glutamate: a missing methylene unit. The schematics in Fig. 6 (*A* and *B*) summarize our interpretation of the pH dependence. The basis of our model is the assumption that the glutamate and the histidine, present in the double mutant, form a salt bridge. Under optimal conditions for hydrolysis, this salt bridge restricts the conformational flexibility of the histidine in a productive orientation. Any changes, for example pH, mutations, etc., that disrupt this interaction will increase the flexibility of the histidine side chain thereby reducing the overall rate of hydrolysis. Such an interaction would also explain the different rates of hydrolysis in the double and in the Q701H mutant. In detail, the double mutant shows a 5-fold higher activity at pH 6.0 than the single mutant at the concentration employed, whereas it is only 2-fold at pH 8.0. In the light of the proposed salt bridges, this behavior is comprehensible,

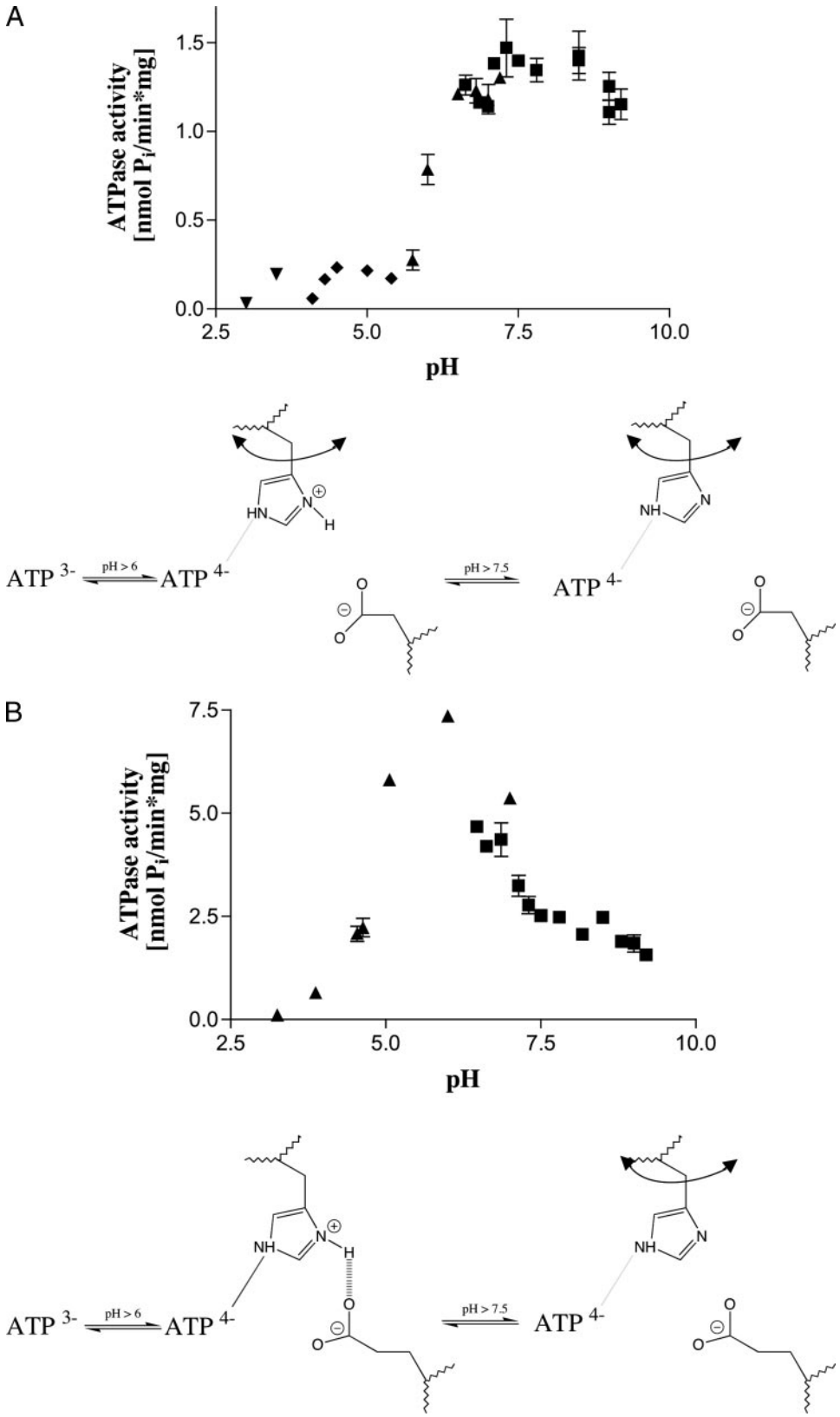

FIGURE 6. *A*, pH dependence of ATPase activity of the Q701H mutant at 30 ± 1 °C and a concentration of 1 mg ml^{-1} (30 μM). The following buffer systems were used: Tris/HCl (*squares*), cacodylate (*triangles*), glycine (*inverted triangles*), and acetate (*diamond*). Data points represent the average of two independent experiments with the standard deviation reported as errors. *B*, pH dependence of ATPase activity of the D668E/Q701H mutant at 30 ± 1 °C and a concentration of 1 mg ml^{-1} (30 μM). Tris/HCl (*squares*) and malonate (*triangles*) were used as buffers. Data points represent the average of two independent experiments with the standard deviation reported as errors. The chemical schematics explain potential interactions of the catalytically relevant amino acids. The *arrow* is placed to suggest a higher flexibility of the histidine side chain in the absence of proper stabilization, *i.e.* in the presence of an aspartate (*A*), where the distance is too large for an effective interaction, or high pH (*B*), which results in deprotonation of the imidazole side chain and consequently a loss of interaction.

because pH changes will affect the protonation state of the histidine and therefore influence the thermodynamic strength of this salt bridge, which is directly related to enzymatic activity. Increasing pH will simply disrupt the proposed salt bridge. In this situation, the double mutant will behave like the Q701H mutant, which is evident from Fig. 6. On the other hand, the latter mutant will not reach the activity levels of the double mutant, because the structural, stabilizing effect of the glutamate is not present, which fixes the side chain of the histidine in a productive and hydrolysis-competent conformation (indicated by the *arrow* in Fig. 6*B*). Further support for this proposal comes from the fact that the pK_a value of a histidine fixed in a salt bridge has been determined experimentally to pH values ~8, which is in accordance with the activity profile of the double mutant (63).

But do these observations really rule out the existence of a catalytic carboxylate? For example, one could envision that the histidine activates the aspartate (Q701H) or the glutamate (double mutant) and therefore induces different levels of ATPase activity in a distance-dependent manner. ATPase activity of the Q701H mutant raises around pH 6.0, peaks around pH 7.0, and remains constant up to pH 10. On a molecular level, this dependence can be explained by the formation of a salt bridge between the protonated histidine and the deprotonated aspartate. This interaction would position the carboxylate in the proper location and conformation for catalysis. If this interpretation is valid, the pH dependence of the double mutant should be qualitatively identical or similar to the Q701H mutant. Obviously, this is not the case. The double mutant displays a bell-shaped dependence, which peaks around pH 7.0 and falls off to the activity levels of the Q701H mutant. Because an activation of the glutamate by the histidine in the double mutant should follow the same molecular principles outlined for the Q701H mutant, this distinction allows us to rule out a scenario, in which the histidine activates the carboxylate. Rather the inverse situation explained above is occurring in the TAP1-NBD. Thus, a catalytic dyad composed of the glutamate and histidine, which are connected by a salt bridge (30), is operational in the engineered double mutant of TAP1-NBDs. Additionally, our data suggest that mutational studies in ABC cassettes should be evaluated over a broader pH range, because the different activities of the Q701H and the double mutant range from 2- to 5-fold in a strongly pH-dependent manner. However, we observed that not only the ATPase activity itself, but also the dimerization of the NBDs strongly depends on the pH. The optimal pH for the hydrolysis of ATP clearly disfavored the dimerization of the hTAP1-NBD by lowering the affinity of the monomers to each other. Thus, the low activity at pH 8 (0.06 ATP/min, Fig. 4*B*) can be raised *drastically* by performing the ATPase assay at pH 6 and by increasing protein concentration even further (data not shown). However, because we wanted to dissect the respective role of two catalytically relevant amino acids, we had to choose an assay to analyze the behavior with respect to hydrolysis and dimerization under identical conditions. Only this allows a direct unbiased comparison of the enzymes employed here and explains the relatively low activity for the double mutant.

Finally, our model can explain the recent report on the asymmetric behavior of the motor domains of the ABC-transporter LmrCD from *L. lactis* (50). Due to the nature of the amino acids forming the catalytic dyad (aspartate/glutamine in LmrC and glutamate/histidine in LmrD), ATPase activity should be asymmetric. Accordingly, LmrC would display no detectable activity, whereas LmrD should be capable of hydrolyzing ATP. This is exactly reflected in the biochemical and mutational studies of the heterodimeric LmrCD complex (50). However, we like to stress here, that further systems have to be investigated before a generalization can be drawn. For HlyB-NBD (30, 41) and for the non-physiological TAP1-NBD homodimer (this study) a catalytic dyad was demonstrated, whereas other studies highlighted the importance of the glutamate (see, *e.g.* Refs. 32, 34, 36–39, and 42). Thus, it is obvious that more ABC-transporters have to be investigated in detail before a final, universal mechanism can be proposed for the whole family of these membrane transporters, assuming that such a mechanism exists at all.

CONCLUSIONS

TAP1 displays sequence degeneration at two positions, which are in contrast highly conserved among ABC-transporters. These two amino acids, aspartate and glutamine, correspond to a glutamate and histidine in the overwhelming majority of ABC cassettes and have been proposed to play a vital role during the catalytic cycle. The mutational studies of TAP1-NBD presented here, now dissect the individual, molecular roles of these key amino acids; introducing either the conserved glutamate or the histidine resulted in mutant proteins with fundamental different activities. Although the glutamate mutant (D668E) remained inactive, ATPase activity was detected in the histidine mutant (Q701H). The histidine of the H-loop is of prime importance during catalysis and is directly involved in the bond-breaking reaction. Thus, in the engineered TAP1-NBD mutant, the glutamate is not of immediate catalytic importance but serves as an important platform to align the histidine in a proper conformation. The fact that the double mutant showed an activity of up to 5-fold higher than the single histidine mutant implies a more structural role for the glutamate. Furthermore, our activity data demonstrated that the engineered ATPase activity stems from a dimeric form of the protein. *In vivo*, the TAP transporter is a heterodimer composed of TAP1 and TAP2 and homodimerization is excluded. However, the data obtained from ATPase activity measurements of the isolated TAP1-NBD are informative from a mechanistic point of view. For the first time it is now possible to distinguish the molecular roles of the glutamate and the histidine and derive important conclusions with respect to the hierarchy of these two amino acids.

Acknowledgments—We thank Jelena Zaitseva, Stefan Jenewein, and Olga Frolow for stimulating discussions and assistance.

REFERENCES

1. Higgins, C. F. (1992) *Annu. Rev. Cell Biol.* **8,** 67–113
2. Blight, M. A., and Holland, I. B. (1994) *Trends Biotechnol.* **12,** 450–455
3. Schmitt, L., and Tampé, R. (2002) *Cur. Opin. Struct. Biol.* **12,** 754–760

4. Jones, P. M., and George, A. M. (2004) *Cell Mol. Life Sci.* **61,** 682–699
5. Holland, I. B., Schmitt, L., and Young, J. (2005) *Mol. Membr. Biol.* **22,** 29–39
6. Schmitt, L., and Tampe, R. (2000) *Chembiochem* **1,** 16–35
7. Pamer, E., and Cresswell, P. (1998) *Annu. Rev. Immunol.* **16,** 323–358
8. Coux, O., Tanaka, K., and Goldberg, A. L. (1996) *Annu. Rev. Biochem.* **65,** 801–847
9. York, I. A., and Rock, K. L. (1996) *Annu. Rev. Immunol.* **14,** 369–396
10. van Endert, P. M., Tampé, R., Meyer, T. H., Tisch, R., Bach, J. F., and McDevitt, H. O. (1994) *Immunity* **1,** 491–500
11. Arora, S., Lapinski, P. E., and Raghavan, M. (2001) *Proc. Natl. Acad. Sci. U. S. A.* **98,** 7241–7246
12. Karttunen, J. T., Lehner, P. J., Gupta, S. S., Hewitt, E. W., and Cresswell, P. (2001) *Proc. Natl. Acad. Sci. U. S. A.* **98,** 7431–7436
13. Lapinski, P. E., Neubig, R. R., and Raghavan, M. (2001) *J. Biol. Chem.* **276,** 7526–7533
14. Chen, M., Abele, R., and Tampe, R. (2003) *J. Biol. Chem.* **278,** 29686–29692
15. Alberts, P., Daumke, O., Deverson, E. V., Howard, J. C., and Knittler, M. R. (2001) *Curr. Biol.* **11,** 242–251
16. Chen, M., Abele, R., and Tampe, R. (2004) *J. Biol. Chem.* **279,** 46073–46081
17. Daumke, O., and Knittler, M. R. (2001) *Eur. J. Biochem.* **268,** 4776–4786
18. Aleksandrov, L., Aleksandrov, A. A., Chang, X. B., and Riordan, J. R. (2002) *J. Biol. Chem.* **277,** 15419–15425
19. Gao, M., Cui, H. R., Loe, D. W., Grant, C. E., Almquist, K. C., Cole, S. P., and Deeley, R. G. (2000) *J. Biol. Chem.* **275,** 13098–13108
20. Hou, Y., Cui, L., Riordan, J. R., and Chang, X. (2000) *J. Biol. Chem.* **275,** 20280–20287
21. Hou, Y. X., Cui, L., Riordan, J. R., and Chang, X. B. (2002) *J. Biol. Chem.* **277,** 5110–5119
22. Chang, G. (2003) *J. Mol. Biol.* **330,** 419–430
23. Chang, G., and Roth, C. B. (2001) *Science* **293,** 1793–1800
24. Locher, K. P., Lee, A. T., and Rees, D. C. (2002) *Science* **296,** 1091–1098
25. Reyes, C. L., and Chang, G. (2005) *Science* **308,** 1028–1031
26. Oswald, C., Holland, I. B., and Schmitt, L. (2006) *Naunyn-Schmiedeberg's Arch. Pharmacol.* **372,** 385–399
27. Ye, J., Osborne, A. R., Groll, M., and Rapoport, T. A. (2004) *Biochim. Biophys. Acta* **1659,** 1–18
28. Chen, J., Lu, G., Lin, J., Davidson, A. L., and Quiocho, F. A. (2003) *Mol. Cell* **12,** 651–661
29. Smith, P. C., Karpowich, N., Millen, L., Moody, J. E., Rosen, J., Thomas, P. J., and Hunt, J. F. (2002) *Mol. Cell* **10,** 139–149
30. Zaitseva, J., Jenewein, S., Jumpertz, T., Holland, I. B., and Schmitt, L. (2005) *EMBO J.* **24,** 1901–1910
31. Davidson, A. L., and Sharma, S. (1997) *J. Bacteriol.* **179,** 5458–5464
32. Moody, J. E., Millen, L., Binns, D., Hunt, J. F., and Thomas, P. J. (2002) *J. Biol. Chem.* **277,** 21111–21114
33. Shyamala, V., Baichwal, V., Beall, E., and Ames, G. F. (1991) *J. Biol. Chem.* **266,** 18714–18719
34. Orelle, C., Dalmas, O., Gros, P., Di Pietro, A., and Jault, J. M. (2003) *J. Biol. Chem.* **278,** 47002–47008
35. Geourjon, C., Orelle, C., Steinfels, E., Blanchet, C., Deleage, G., Di Pietro, A., and Jault, J. M. (2001) *Trends Biochem. Sci.* **26,** 539–544
36. Janas, E., Hofacker, M., Chen, M., Gompf, S., van der Does, C., and Tampe, R. (2003) *J. Biol. Chem.* **278,** 26862–26869
37. Sauna, Z. E., Muller, M., Peng, X. H., and Ambudkar, S. V. (2002) *Biochemistry* **41,** 13989–14000
38. Tombline, G., Bartholomew, L. A., Tyndall, G. A., Gimi, K., Urbatsch, I. L., and Senior, A. E. (2004) *J. Biol. Chem.* **279,** 46518–46526
39. Urbatsch, I. L., Julien, M., Carrier, I., Rousseau, M. E., Cayrol, R., and Gros, P. (2000) *Biochemistry* **39,** 14138–14149
40. Verdon, G., Albers, S. V., van Oosterwijk, N., Dijkstra, B. W., Driessen, A. J., and Thunnissen, A. M. (2003) *J. Mol. Biol.* **334,** 255–267
41. Zaitseva, J., Jenewein, S., Wiedenmann, A., Benabdelhak, H., Holland, I. B., and Schmitt, L. (2005) *Biochemistry* **44,** 9680–9690
42. Payen, L. F., Gao, M., Westlake, C. J., Cole, S. P., and Deeley, R. G. (2003) *J. Biol. Chem.* **278,** 38537–38547
43. Nikaido, K., and Ames, G. F. (1999) *J. Biol. Chem.* **274,** 26727–26735
44. Schweins, T., Geyer, M., Scheffzek, K., Warshel, A., Kalbitzer, H. R., and Wittinghofer, A. (1995) *Nat. Struct. Biol.* **2,** 36–44
45. Saveanu, L., Daniel, S., and van Endert, P. M. (2001) *J. Biol. Chem.* **276,** 22107–22113
46. Zaitseva, J., Zhang, H., Binnie, R. A., and Hermodson, M. (1996) *Protein Sci.* **5,** 1100–1107
47. Horn, C., Bremer, E., and Schmitt, L. (2003) *J. Mol. Biol.* **334,** 403–419
48. Faller, L. D. (1989) *Biochemistry* **28,** 6771–6778
49. Faller, L. D. (1990) *Biochemistry* **29,** 3179–3186
50. Lubelski, J., van Merkerk, R., Konings, W. N., and Driessen, A. J. (2006) *Biochemistry* **45,** 648–656
51. Gaudet, R., and Wiley, D. C. (2001) *EMBO J.* **20,** 4964–4972
52. Mildvan, A. S. (2004) *Biochemistry* **43,** 14517–14520
53. Schneider, E., and Hunke, S. (1998) *FEMS Microbiol. Rev.* **22,** 1–20
54. Delepelaire, P. (1994) *J. Biol. Chem.* **269,** 27952–27957
55. Ramaen, O., Masscheleyn, S., Duffieux, F., Pamlard, O., Oberkampf, M., Lallemand, J. Y., Stoven, V., and Jacquet, E. (2003) *Biochem. J.* **376,** 749–756
56. Nikaido, K., Liu, P. Q., and Ames, G. F. (1997) *J. Biol. Chem.* **272,** 27745–27752
57. Ramaen, O., Leulliot, N., Sizun, C., Ulryck, N., Pamlard, O., Lallemand, J. Y., Tilbeurgh, H. V., and Jacquet, E. (2006) *J. Mol. Biol.* **359,** 940–949
58. Sauna, Z. E., Smith, M. M., Muller, M., Kerr, K. M., and Ambudkar, S. V. (2001) *J. Bioenerg. Biomembr.* **33,** 481–491
59. Fetch, E. E., and Davidson, A. L. (2002) *Proc. Natl. Acad. Sci. U. S. A.* **99,** 9685–9690
60. Gadsby, D. C., Vergani, P., and Csanady, L. (2006) *Nature* **440,** 477–483
61. Vergani, P., Lockless, S. W., Nairn, A. C., and Gadsby, D. C. (2005) *Nature* **433,** 876–880
62. van der Does, C., Presenti, C., Schulze, K., Dinkelaker, S., and Tampe, R. (2006) *J. Biol. Chem.* **281,** 5694–5701
63. Yang, J., Yu, M., Jan, Y. N., and Jan, L. Y. (1997) *Proc. Natl. Acad. Sci. U. S. A.* **94,** 1568–1572